Chinese Journal of Aeronautics, (2015), 28(6): 1725–1734

Chinese Society of Aeronautics and Astronautics
& Beihang University

Chinese Journal of Aeronautics

cja@buaa.edu.cn
www.sciencedirect.com

A novel particle filter approach for indoor positioning by fusing WiFi and inertial sensors

Zhu Nan, Zhao Hongbo *, Feng Wenquan, Wang Zulin

School of Electronics and Information Engineering, Beihang University, Beijing 100191, China

Received 12 December 2014; revised 24 July 2015; accepted 7 August 2015
Available online 19 October 2015

KEYWORDS

Fusion algorithm;
Indoor positioning;
Inertial sensor;
Rao Blackwellized particle filter;
WiFi fingerprinting

Abstract WiFi fingerprinting is the method of recording WiFi signal strength from access points (AP) along with the positions at which they were recorded, and later matching those to new measurements for indoor positioning. Inertial positioning utilizes the accelerometer and gyroscopes for pedestrian positioning. However, both methods have their limitations, such as the WiFi fluctuations and the accumulative error of inertial sensors. Usually, the filtering method is used for integrating the two approaches to achieve better location accuracy. In the real environments, especially in the indoor field, the APs could be sparse and short range. To overcome the limitations, a novel particle filter approach based on Rao Blackwellized particle filter (RBPF) is presented in this paper. The indoor environment is divided into several local maps, which are assumed to be independent of each other. The local areas are estimated by the local particle filter, whereas the global areas are combined by the global particle filter. The algorithm has been investigated by real field trials using a WiFi tablet on hand with an inertial sensor on foot. It could be concluded that the proposed method reduces the complexity of the positioning algorithm obviously, as well as offers a significant improvement in position accuracy compared to other conventional algorithms, allowing indoor positioning error below 1.2 m.
Crown Copyright © 2015 Published by Elsevier Ltd. This is an open access article under the CC BY-NC-ND license (http://creativecommons.org/licenses/by-nc-nd/4.0/).

1. Introduction

Global navigation satellite system (GNSS) could provide accurate positioning in the outdoor environment.[1] However, the limitation of signal propagation makes this technology difficult for indoor positioning. Therefore, various systems offering high performance for indoor localization have been proposed. Due to the popularity and wide spread inside building, WiFi positioning was recently introduced as a potential alternative to GNSS in satellite signal denied areas.

In WiFi networks, the principal source of information is the received signal strength (RSS). WiFi positioning requires the use of a propagation model which describes the change in RSS with distance. The log fading model is widely used for this purpose. Recently, for indoor positioning, the prevalent technique is WiFi fingerprinting, which requires the database creation of RSS values from each access point (AP).[2] When positioning, user's device records its own value of RSS and

* Corresponding author. Tel.: +86 10 82317210.
E-mail address: bhzhb@buaa.edu.cn (H. Zhao).
Peer review under responsibility of Editorial Committee of CJA.

Production and hosting by Elsevier

http://dx.doi.org/10.1016/j.cja.2015.09.009
1000-9361 Crown Copyright © 2015 Published by Elsevier Ltd.
This is an open access article under the CC BY-NC-ND license (http://creativecommons.org/licenses/by-nc-nd/4.0/).

matches it against the pre-recorded database. Location is then calculated based on good matches between new and stored values. The accuracy depends on the number of positions registered in the database. Besides, signal fluctuations over time could induce errors and discontinuities in the user's trajectory. In Ref.[3], an energy efficient WiFi indoor positioning algorithm is proposed, using the probabilistic fingerprinting method, to eliminate the fluctuations. Hybrid positioning systems were employed to enhance the performance of WiFi indoor positioning in Ref.[4]. Furthermore, the collaborative RSS fingerprinting system was utilized to overcome the cost and time-consuming problem of WiFi RSS positioning in Ref.[5].

To minimize the fluctuation of RSS, other methods such as the low-cost inertial sensors have been used. Due to their complementary advantages, fusing both systems could increase the positioning accuracy.[6] Pedestrian step is detected by the inertial sensors and the estimated walking direction and step length are fed into the particle filter as a motion model to predict the new particles. The weight of the particle is updated by computing the distance between the particle and the WiFi localization result.[7] Ref.[8] presents a sequential importance resampling particle filter to fuse the accelerometer and WiFi signals. Also, an augmented particle filter is proposed to simultaneously estimate location, step length and user heading. The user heading could be estimated by the inertial sensor, then updated by the user's trajectory in the measurement model of the augmented particle filter.[9] Inspired by our previous study on inertial positioning, the pedestrian heading could be obtained by the principle heading of building on map.[10]

Theoretically, for indoor positioning, Particle filter (PF) can be employed for any state model, but the major disadvantage of PF is that sampling in high dimensional states can be inefficient.[11–13] For large area mapping, some approaches divide the whole environment into several sub-areas which are estimated independently, and then these local maps are joined through a global optimization algorithms.[14,15]

This paper proposes a novel particle filter approach for indoor positioning by fusing WiFi and inertial sensors. The measurement model is developed using WiFi fingerprinting, which accurately characterizes the RSS relation and could measure the related noise. For the state model, the heading information and the step length could be computed by fusing the accelerometer and gyroscopes. In the proposed algorithm, local areas are estimated independently by a local filter, and then the trajectory of the local map origin is estimated by a global filter. So the implementation of proposed Rao Blackwellized particle filter (RBPF) for indoor positioning could not only induce the complexity reduction, but also offer better accuracy compared to other conventional algorithms.

The remaining sections of this paper are organized as follows: Section 2 presents the basic techniques of pedestrian inertial sensor. The WiFi-based measurement method is described in Sections 3 and 4 demonstrates the proposed RBPF algorithm. Section 5 gives the trial setup and preliminary results. Finally, the conclusion is drawn in Section 6.

2. Pedestrian inertial sensor method

Fig. 1 presents the architecture of the proposed fusion approach. The proposed method takes the WiFi RSS sensors and inertial sensors as input and outputs the user's location upon each step.

The algorithm includes three major components: inertial sensors, WiFi RSS and the RBPF. Inertial segment computes the steps of the user and the length of each step. It also calculates the heading information aided by building layout, as illustrated in our previous study.[10] The pedestrian motion vector, [length, direction, time], would pass to RBPF as the state model.

WiFi RSS records values periodically from all Aps as a RSS vector of [rss1, rss2, rss3, . . ., time]. WiFi fluctuations could cause notable variety in RSS vectors. The behavior of user turning and entering room could mislead the inertial sensor, due to the insufficient scanning of low-cost inertial sensor. So the algorithm contains the turn distinguishing and entrance discovering, as illustrated in Section 3.

PF method redistributes each particle according to the pedestrian state at the particle propagation phase. At the correcting phase, the algorithm corrects the weight of each particle according to the map and calculates the center of the particles. Finally, in the resampling phase, the new center of weighted particles is output as the current estimated position.

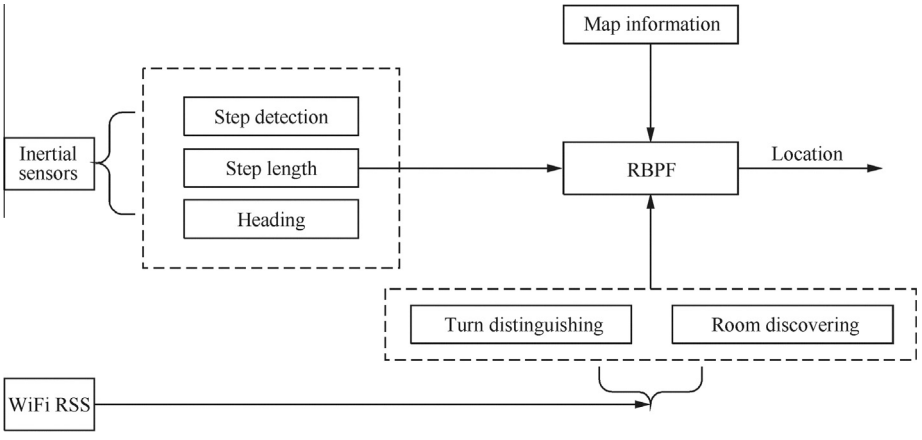

Fig. 1 Architecture of the proposed fusion approach.

2.1. Zero velocity update

Zero velocity update (ZUPT) is one of the main improvements available for pedestrian navigation and it is based on the physical property. During walking, the foot has to be briefly stationary while it is on the ground and at this time the foot does not have any velocity.[16] Therefore, the non-zero velocity measurement from the inertial sensors during this period is considered as an error and can be subsequently corrected. Furthermore if this zero velocity measurement is used in Kalman filter, as adopted in this paper, it could not only correct the user's velocity, but also restrict the position error. ZUPT is applied during each detected stance phase of the walking, so the inertial errors are allowed to grow only between these ZUPTs. Fig. 2 shows an example of detected ZUPT during a walk and reveals that the algorithm is quite reliable.

However, there remains the unobservable heading error that could cause the position drift. Because the heading of the inertial sensor does not affect the velocity, ZUPT measurements are unable to restrict the error. The relationship between velocity errors and attitude errors in local level frame is shown in Eqs. (1)–(3):

$$\dot{\boldsymbol{\delta}}_{V_N} = -\boldsymbol{f}_D \varepsilon_\theta + \boldsymbol{f}_E \varepsilon_\varphi \tag{1}$$

$$\dot{\boldsymbol{\delta}}_{V_E} = \boldsymbol{f}_D \varepsilon_\phi - \boldsymbol{f}_N \varepsilon_\varphi \tag{2}$$

$$\dot{\boldsymbol{\delta}}_{V_D} = -\boldsymbol{f}_E \varepsilon_\phi + \boldsymbol{f}_N \varepsilon_\theta \tag{3}$$

where $\boldsymbol{f}$ is the force in the local frame and ε_ϕ, ε_θ, ε_φ are the roll, pitch and yaw errors respectively. During ZUPT, the horizontal forces $\boldsymbol{f}_E$ and $\boldsymbol{f}_N$ in the local frame are basically zero and specific force $\boldsymbol{f}_D$ in the downward direction is approximately close to the negative gravity constant. Therefore, the above equations show that ε_ϕ and ε_θ could result in the velocity errors $\dot{\boldsymbol{\delta}}_{V_N}$, $\dot{\boldsymbol{\delta}}_{V_E}$ and $\dot{\boldsymbol{\delta}}_{V_D}$, so ε_ϕ and ε_θ are always observable. However, the yaw error ε_φ is only observable by $\dot{\boldsymbol{\delta}}_{V_E}$ and $\dot{\boldsymbol{\delta}}_{V_N}$, In order to observe ε_φ, the horizontal acceleration should not be zero, which is impossible when using ZUPT. Therefore, the error ε_φ becomes the crucial factor of heading drift.[17]

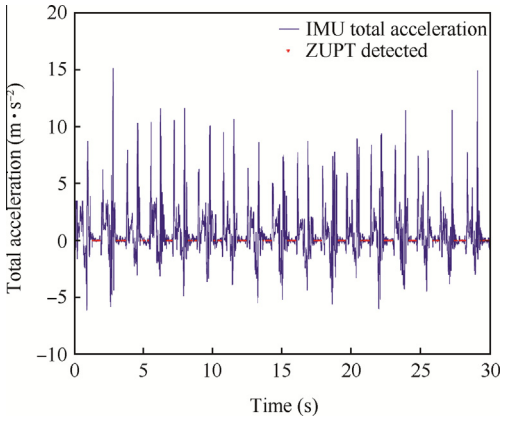

Fig. 2 ZUPT detection results.

2.2. Building aiding measurements

Building aiding measurements are obtained by extracting the principle heading of individual building on a map. After that, the heading measurements will update the filter. This algorithm will be shown as follows, to significantly reduce the heading drift of the low-cost INS and make the initialization efficient.

The algorithm is based on two important assumptions. Firstly, it is assumed that the pedestrians tend to be constrained to a heading direction, which lies parallel to be the outside of the building.[18] Secondly, it is assumed that the difference between the step and the outer orientation of the building is the result of heading drift plus some uncertainty resulting from the pedestrian not walking in a straight line.[19] Due to the acceleration, the heading error is observable through the position difference, as heading is used to determine the orientation of the accelerometer axes. This algorithm will be entirely based on a simple illustration drawn in Fig. 3.

Step length d is computed based on the changes in horizontal position (north and east):

$$d = \sqrt{d_N^2 + d_E^2} \tag{4}$$

The algorithm continues by making computation of a step heading φ_{step}:

$$\varphi_{step} = \arctan \frac{d_E}{d_N} \tag{5}$$

The step heading is defined as the angle between two successive steps and it is calculated at each ZUPT epoch. φ_{step} is the measured step heading; d_E and d_N are the changes in east and north.[20]

The measurement update is applied by forming the observation equation as follows:

$$\varphi_{error} = \varphi_{building} - \varphi_{step} \tag{6}$$

where φ_{error} is the INS heading error, and $\varphi_{building}$ the current building orientation.

$$\varphi_{error} = \left[\frac{\partial\varphi}{\partial\varepsilon_\phi}, \frac{\partial\varphi}{\partial\varepsilon_\theta}, \frac{\partial\varphi}{\partial\varepsilon_\varphi}\right] \left[\varepsilon_\phi, \varepsilon_\theta, \varepsilon_\varphi\right]^T + n_k \tag{7}$$

where n_k is the measurement noise at kth epoch, and it represents the uncertainties when a pedestrian does not walk in straight lines with respect to building orientations.

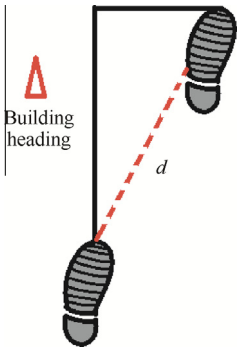

Fig. 3 Sample of heading algorithm.

3. WiFi measurement

Inertial sensors could obtain relative displacement with high accuracy in a short period. However, it suffers from accumulative drift errors during walking. WiFi-based positioning system could provide the absolute location estimation, while it sustains the loss of accuracy when significant RSS fluctuations happen. By fusing the two methods, it would exploit their complementary advantages.[21]

Fingerprinting method consists of some signal power footprints or signatures that define the position in the environment. This signature is made of the received signal powers from different APs that cover the environment. WiFi fingerprinting method requires much more preparation time, however potentially gives more accurate positioning results.[22] Also, even the AP redeployment in the same room could make the fingerprint database different. Fig. 4 presents the measurements recorded in RSS vectors during pedestrian walking from A to B. It shows that the closer a pedestrian walks to the AP,

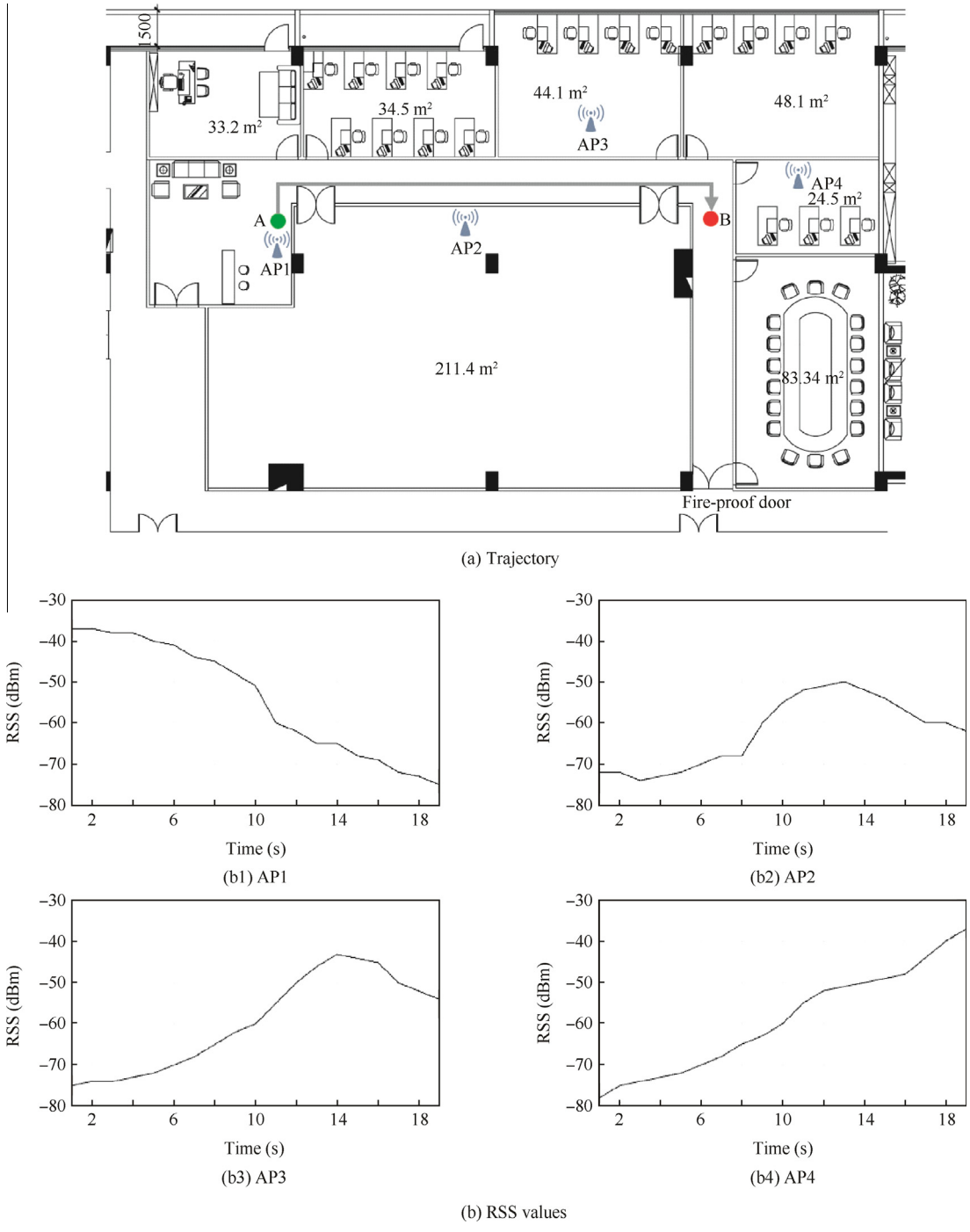

Fig. 4 Measurement of RSS while walking.

the higher RSS values are obtained. Also, there exist some fluctuations in RSS values, which would be elaborated as follows.

3.1. Turn distinguishing

The WiFi method suffers from the fluctuation of RSS, mainly due to the instable channel and human behavior. The fluctuations could induce the algorithm to continuously choose a different position for the user even not moving or turning. So reducing the unexpected jumps is necessary to improve the rough positioning.

When the pedestrian walks, unconscious human behavior, such as hand trembling, would mislead the WiFi sensors.[23] If such wrong estimation is not corrected, huge position errors would appear when two methods fused.

Turn distinguishing algorithm is proposed to eliminate the effect. When examining RSS vectors from each AP between continuous steps, we choose the highest RSS values from the unique AP. Then we use the chosen vector direction to confirm whether the turn behavior occurs. If the angle of two consecutive RSS vectors is higher than a threshold defined before, the turn behavior would be affirmed. Otherwise, the heading direction would be replaced by previous step, as no turn exists in motion. The algorithm is illustrated as follows.

3.2. Room discovering

Input: t_c, t_{p1}, t_{p2} // t_c, t_{p1}, t_{p2}: current and last two epochs
V_c, V_p //V_c, V_p: current and last vector
Output: Current heading direction
$\phi = \arccos(V_c, V_p)/(|V_c|.|V_p|)$
If $\phi \in (\pi/4, 3\pi/4)$ **then**
return Current heading direction = V_c
else
return Current heading direction = V_p
End if

When a pedestrian enters a room, we could find a clear tendency in the change of RSS vectors and the particles should follow the motion. However, in real environments, the number of particles is limited to typically 300, thus the distribution is of radius 1 m, only covers half of the corridor. Therefore, there could exist the situation that when people enter a room through the door, particles keep dying with the position estimated against the wall, as shown in Fig. 5(a) and (b). To alleviate that dilemma, the RSS vectors are utilized. If the RSS values keep changing, the pedestrian should not be static and move into the room. Then the algorithm queries the map to locate the nearest door between the founded AP and current position. The particle would be resampled with the weight 1, while all other particles would be deleted. Thus pedestrian motion estimated should be accurate after the resampling phase, as shown in Fig. 5(c).

4. RBPF algorithm

PF algorithm receives the motion vector [length, direction, time] from inertial sensors, and fuses with the WiFi RSS vector [rss1, rss2, rss3, ..., time], then outputs localization result. The particles are initialized as follows:

$$P_t = \{\langle p_t^i, w_t^i \rangle\}, \quad i = 1, 2, \ldots, N \tag{8}$$

$$p_t^i = (x_t^i, y_t^i, \theta_t^i) \tag{9}$$

where p_t^i is the estimated position with weight w_t^i of i particle at epoch t, N is the whole numbers of the particles, while θ_t^i denotes the heading information.

As the WiFi sensor could be sparse and short in range, the whole region is divided into several local areas as shown in Fig. 6.

The global map is divided into 4 local maps according to the pedestrian trajectory. The local map and global map are hierarchically estimated by RBPF. The algorithm is based on three assumptions as follows[24]:

(1) The local maps are independent of each other.
(2) The global estimates are independent of raw data which is used for local maps.
(3) Indoor environments mainly consist of orthogonal line.

The third assumption is the same as the requirements of the building aiding measurements used in Section 2.2. Thus, we could define the map as follows:

$$m = \{M, m^{1:\tau}\} \tag{10}$$

where M and $m^{1:\tau}$ represent global and local maps; τ indicates the number of local maps.

The whole process of RBPF algorithm is shown in Fig. 7. Firstly, pedestrian walks in a local area, while processing by the local RBPF. Secondly, after closing loop for the local

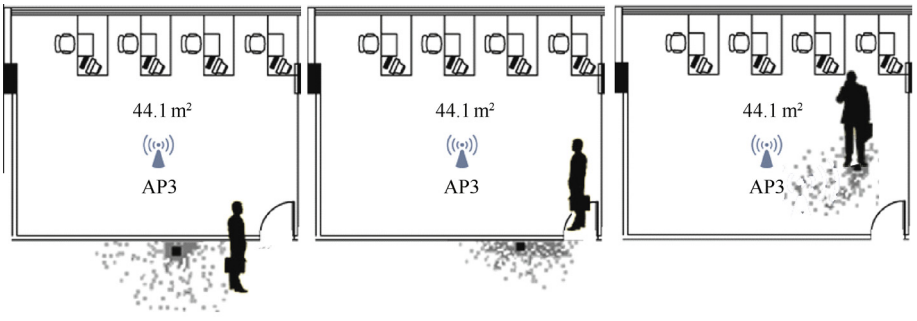

(a) Condition 1 (b) Condition 2 (c) Condition 3

Fig. 5 Room discovering.

region, the local particles are merged into a single map and used in the global RBPF for measurement update. Thirdly, pedestrian walks into another local area and the localization particles are used as the sample distribution for updating the distribution in global RBPF. The whole process would iterate until the global map closure detected.

4.1. Local RBPF

Local RBPF is processed in the margin of local area. The particle p_t^i is generated through three steps as follows:

4.1.1. Particle propagation

The new location and heading of the i particle at step t are

$$\theta_t^i = \varphi_t + \varepsilon \tag{11}$$

$$x_t^i = x_{t-1}^i + (l_t + \delta)\cos\theta_t \tag{12}$$

$$y_t^i = y_{t-1}^i + (l_t + \delta)\sin\theta_t \tag{13}$$

where φ_t is the step direction, and l_t denotes the stride length; δ and ε are zero-Gaussian noises for stride length and heading respectively.

4.1.2. Particle correction

This step is to correct the weights of propagated particles. Due to the boundary of local map, if the particle moves across the wall, the weight would be given to zero. The weights are updated as

$$w_t^i = \frac{w_{t-1}^i}{\sum_{i\in P_t} w_{t-1}^i} \tag{14}$$

Correction process will interact with WiFi component under particular conditions, such as the turn distinguishing and room discovering.

4.1.3. Resampling

The step is to delete the particles with weight 0 and regenerate new ones for the surviving particles. The weighted center of all particles would be computed again and the current estimated position is output.

4.2. Global RBPF

Global RBPF estimates the global area using the trajectory of local map. Every particle contains the unique global map estimation; however, it would increase the computation. So we alleviate the burden with all particles sharing local maps and the corresponding vectors. Thus the particles would include trajectories and weights only:

$$P_\tau^i = \{\langle \xi_{1:\tau}^i, w_\tau^i \rangle\} \tag{15}$$

$$M_\tau = \{\langle m_{1:\tau}, \boldsymbol{V}_{1:\tau} \rangle\} \tag{16}$$

where $\xi_{1:\tau}^i$ the trajectory of local map, w_τ^i the particle weight and $\boldsymbol{V}$ the vector in local map m.

Then we could process the global RBPF as follows.

Input: p_t^i // p_t^i: local particle
$P_{\tau-1}^i$ // $P_{\tau-1}^i$: previous global particle
Output: P_τ^i // P_τ^i: current global particle
For $i = 1, 2, \ldots, N$
$\xi_\tau^i = \xi_{\tau-1}^i \oplus \xi^i$
End for
return $P_\tau^i = \{\langle \xi_{1:\tau}^i, w_\tau^i \rangle\}$

Firstly, the probability distribution in the local map is input as the localization particle p_t^i; secondly, it combines them to generate new trajectory ξ_τ^i; finally, the algorithm outputs the global particle P_τ^i. [25]

5. Field trial

5.1. Equipmental setup

The experiments were conducted to test the proposed approach. The pedestrian carried a foot mounted Microstrian inertial sensor, with Samsung Galaxy tablet on hand, as shown in Fig. 8. The low cost inertial sensor could induce errors that may result in a large position drift. The sampling frequency of inertial sensor was set at 50 Hz, while the sampling frequency of WiFi sensor was 5 Hz.

The trials were carried out in an indoor office area covering 362.6 m^2, as shown in Fig. 6. There are four APs available and 30 reference points to be deployed. The distance between neighbor reference points is 1.2 m. During offline step, 8 training samples were collected per reference point to build the fingerprint database.

To show the convincing results, 6 pedestrian users were chosen to collect the data of 100 trajectories. The pedestrian moved at a regular walking speed of about 1 m/s, and the trajectory was designed, as shown in Fig. 6, including turn behavior and entering the room with AP3.

5.2. Performance of the proposed fusion method

To confirm the validity of the proposed fusion approach, positioning results with inertial senor and WiFi sensor separately are presented for comparison, as shown in Fig. 9(a). Results with the proposed method and the truth path are shown in Fig. 9(b).

In Fig. 9(a), the black dotted line indicates the path estimated with inertial sensor, while the red dotted line indicates the path estimated with WiFi sensor. There exist critical errors for the inertial sensor. The true trajectory is that the pedestrian entered the room with AP3, through the door, turned backwards and walked out. However, the black path computed by the inertial method, pass the wall into the room. Whereas the red path estimated by the WiFi method, presents accuracy results when entering the room. It is mainly because of the algorithm proposed in Sections 3.1 and 3.2.

Though WiFi localization obtains inaccurate tracking results along the whole path, it could provide useful information, especially along the orthogonal path (Fig. 9(a)). However we find that the WiFi method provides bad results severely,

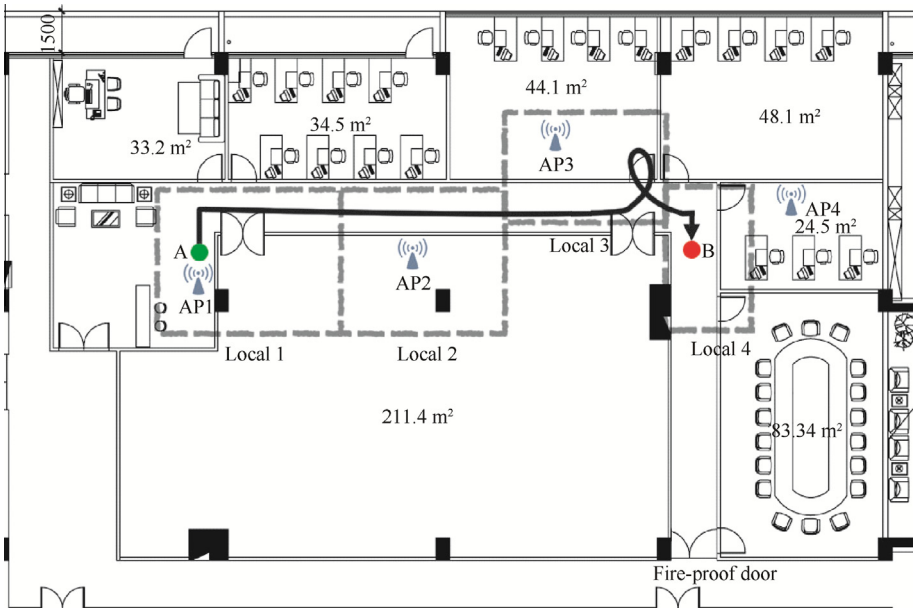

Fig. 6 Local areas and global areas.

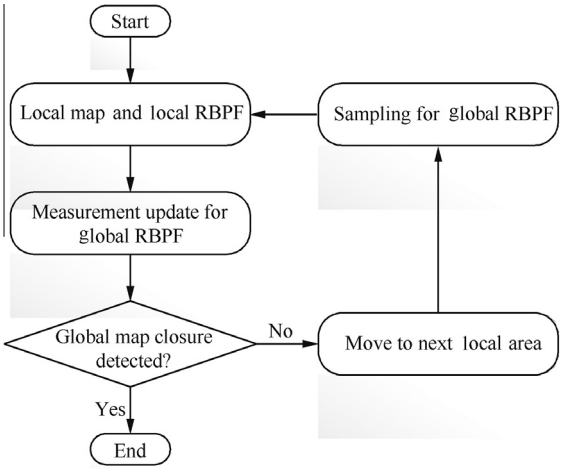

Fig. 7 Flowchart of the proposed RBPF algorithm.

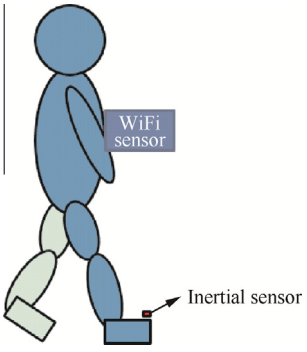

Fig. 8 Positioning equipment setup.

when pedestrian walked in the corner. The estimated location is unacceptably far from the truth.

Clearly, the proposed fusion performs best and provides the estimated trajectories matching the ground truth closest. Turn distinguishing is invoked in the corner, where the highest RSS values from the corresponding AP are found. Then we calculate the vector direction to confirm whether the turn behavior occurs.

After finding that the estimated position against the wall lasts for several epochs, we check whether RSS values keep changing. The room discovering algorithm begins, and it finds the nearest door between AP3 and current position. Then the algorithm corrects the path estimated by resampling the particle. From Fig. 9, it could be indicated that the estimated position reaches the end point B only 0.8 m away from the truth path.

We compare the positioning accuracy among various approaches. As shown in Table 1, compared with inertial sensor and WiFi sensor, the proposed approach performs much better, while it could achieve mean position error by 1.2 m and standard deviation by 0.7 m. The corresponding cumulative error distributions are also shown in Fig. 10. From the figure, we could find that nearly 70% of the error distance is below 1 m, which could achieve the need of indoor positioning accuracy.

5.3. Computation burden

Positioning accuracy could be promoted by increasing particle numbers; however, the computation and storage cost of PF is

Table 1 Position errors.

Position method	Mean error μ(m)	Standard deviation σ(m)
Proposed fusion	1.2	0.7
Inertial sensor	2.1	1.6
WiFi sensor	2.8	2.1

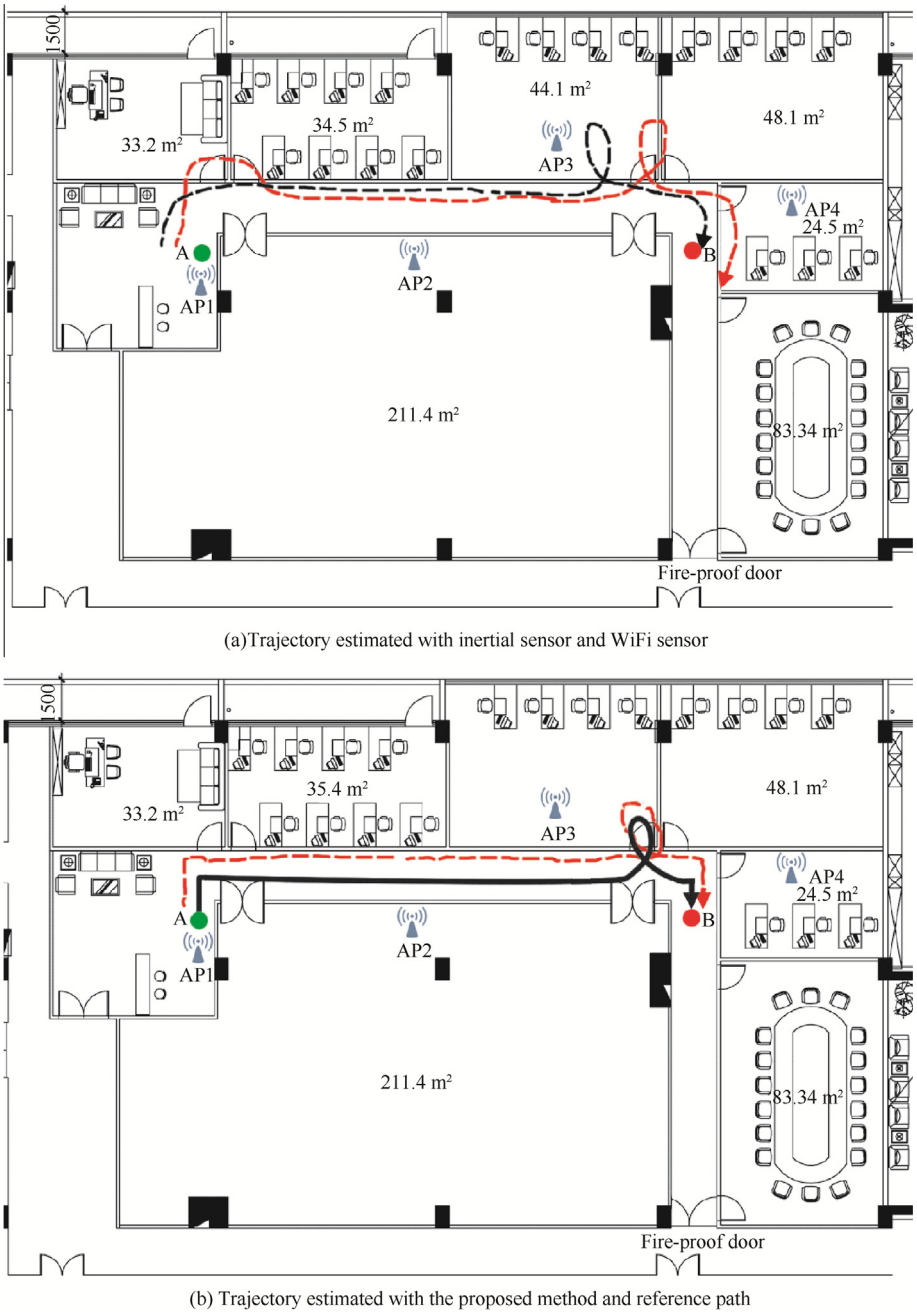

Fig. 9 Trajectory estimated.

proportional to the numbers. Due to the heavy computation burden, large particle-based approach should be run on a server and is unsuitable for real-time applications. Actually, there is a tradeoff between position accuracy and computation burden.

This paper utilizes the local RBPF and global RBPF algorithm to reduce the cost. According to the indoor area, the size of each local area was set to 2.5 m × 3 m. For the local RBPF, only 100 particles were used and reused each time when entering new local area. The particles for global RBPF need relatively little cost because they do not possess their own areas, therefore 300 particles are used for the global RBPF. Thus, after the local RBPF, we approximate the particles as

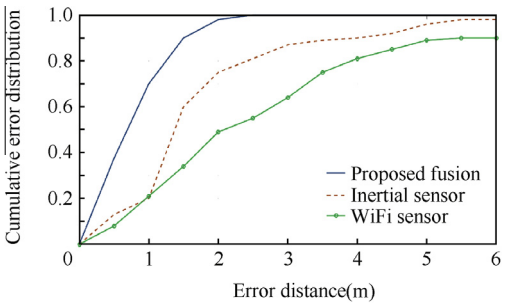

Fig. 10 Accuracy comparison using different methods.

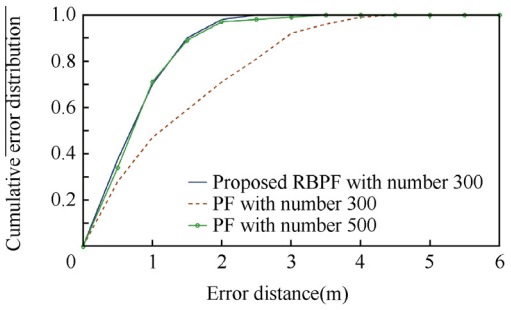

Fig. 11 Accuracy comparison with different numbers.

a Gaussian distribution, and sample 200 more particles to generate the 300 particles.

We compare the positioning accuracy between the proposed RBPF algorithm and the previous PF algorithm. Fig. 11 shows the cumulative error distributions using different particle numbers. We can find that the accuracy degrades severely when using PF algorithm with 300 particles, and only 47% of the error distance is below 1 m. If we enlarge the particle numbers, then the accuracy would increase. Thus, when the particle number is 500, the performance of PF algorithm would achieve comparable accuracy of the proposed RBPF. So it is more suitable for real-time indoor position by the proposed RBPF algorithm.

6. Conclusion

In this paper, a novel fusion algorithm for indoor positioning is proposed. The filter method is exploited to integrate inertial sensor, WiFi sensor and the map information. Also, local RBPF and global RBPF are introduced into the fusion algorithm. By dividing the indoor environments into several local areas, without computing the global areas, the computation could reduce greatly.

Preliminary trial results show that the proposed RBPF algorithm could achieve the positioning accuracy of 1.2 m and it meets the need of indoor positioning. Also, the calculation burden is nearly half of the conventional PF methods.

There remain some problems that should be addressed for practical use. We need to expand the proposed approach to the situation with non-orthogonal environments. Thus, these considerations would be developed in the future work.

Acknowledgments

The trial undertaken for this paper was partly conducted at Nottingham Geospatial Institute at the University of Nottingham, UK. The authors would like to express the sincere gratitude to Dr. Meng for the infinite support and guidance throughout the trial.

References

1. Cobb HS. GPS pseudolites: theory, design, and applications [dissertation]. California: Stanford University; 1997.
2. Chen Y, Kobayashi H. Signal strength based indoor geolocation. *IEEE international conference on communications*. New York, USA; 2002 Apr 28–May 02; 2002. p. 436–9.
3. Bisio I, Lavagetto F, Marchese M. Energy efficient WiFi-based fingerprinting for indoor positioning with smartphones. *Global communications conference (GLOBECOM)*. Atlanta, GA, USA; 2013. p. 4639–43.
4. Bisio I, Lavagetto F, Marchese M. GPS/HPS and Wi-Fi fingerprint-based location recognition for check-in applications over smartphones in cloud-based LBSs. *IEEE Trans Multimedia* 2013;**15**(4):858–69.
5. Kim Y, Chon Y, Cha H. Smartphone-based collaborative and autonomous radio fingerprinting. *IEEE Trans Syst Man Cybern Part C: Appl Rev* 2012;**42**(1):112–22.
6. Evennou F, Marx F. Advanced integration of WiFi and inertial navigation systems for indoor mobile positioning. *Eurasip J Appl Signal Process* 2006(17):1–11.
7. Sun Y, Xu Y, Li C. Kalman/map filtering-aided fast normalized cross correlation-based Wi-Fi fingerprinting location sensing. *J Sens* 2013;**13**(11):15513–31.
8. Wu D, Xia L, Mok E. *Principle and application progress in location-based services*. Switzerland: Springer International Publishing; 2014. p. 81–92.
9. Rai A, Chintalapudi KK, Padmanabhan VN. Zee: zero-effort crowdsourcing for indoor localization. *Proceedings of the 18th annual international conference on mobile computing and networking*. Istanbul, Turkey; 2012 August 22–26; 2012. p. 293–304.
10. Feng W, Zhao H, Zhao Q. Integration of GPS and low cost INS for pedestrian navigation aided by building layout. *Chin J Aeronaut* 2013;**26**(5):1283–9.
11. Gustafsson F, Gunnarsson F, Bergman N. Particle filters for positioning, navigation, and tracking. *IEEE Trans Signal Process* 2002;**50**(2):425–37.
12. Smith A. *Sequential Monte Carlo methods in practice*. 1st ed. New York: Springer; 2013. p. 31–45.
13. Gordon NJ, Salmond DJ, Smith A. Novel approach to nonlinear/non-Gaussian Bayesian state estimation.. *IEE Proc F (Radar Signal Process)* 1993;**140**(2):107–13.
14. Kuo WJ, Tseng SH, Yu JY. A hybrid approach to RBPF based SLAM with grid mapping enhanced by line matching. *International conference on intelligent robots and systems*. St. Louis, MO, USA; 2009 October 10–15; 2009. p. 1523–8.
15. Newman P, Sibley G, Smith M. Navigating, recognizing and describing urban spaces with vision and lasers. *Int J Robotics Res* 2009;**28**(11):1406–33.
16. Feliz AR, Zalama CE, Gómez García-Bermejo J. Pedestrian tracking using inertial sensors. *J Phys Agents* 2009;**3**(1):35–42.
17. Rajagopal S. Personal dead reckoning system with shoe mounted inertial sensors [dissertation]. Sweden: Stockholm University; 2008.
18. Borenstein J, Ojeda L. Heuristic drift elimination for personnel tracking systems. *J Navig* 2010;**63**(4):591–606.
19. Altun K, Barshan B. Pedestrian dead reckoning employing simultaneous activity recognition cues. *J Meas Sci Technol* 2012;**23**(2):103–24.
20. Aggarwal P, Thomas D, Ojeda L. Map matching and heuristic elimination of gyro drift for personal navigation systems in GPS-denied conditions. *J Meas Sci Technol* 2011;**22**(2):205–19.
21. Deng ZA, Hu Y, Yu J. Extended Kalman filter for real time indoor localization by fusing WiFi and smartphone inertial sensors. *J Micromach* 2015;**6**(4):523–43.
22. Smailagic A, Kogan D. Location sensing and privacy in a context-aware computing environment. *J Wireless Commun* 2002;**9**(5):10–7.
23. Hong F, Zhang YT, Zhang Z,Wei MY, Feng Y, Guo ZW. WaP: Indoor localization and tracking using WiFi-assisted particle filter. *2014 IEEE 39th conference on local computer networks*. Edmonton, AB, Canada; 2014 September 8–11; 2014. p. 210–7.
24. Lee T, Lee S, Oh S. A hierarchical RBPF SLAM for mobile robot coverage in indoor environments. *IEEE/RSJ international*

conference on intelligent robots and systems (IROS). San Francisco, CA, USA; 2011 September 25–30; 2011. p. 841–6.
25. Smith R, Self M, Cheeseman P. *Autonomous robot vehicles*. New York: Springer; 1990.

Zhu Nan is a Ph.D. candidate at Beihang University. His current research interests include satellite navigation and signal processing.

Zhao Hongbo received Ph.D. degree in communication and information system from Beihang University in 2012. He has been teaching there since 2012. His current research interests include signal processing, satellite navigation and satellite communication.

Feng Wenquan received Ph.D. degree in communication and information system from Beihang University, Beijing, China. He is a professor and works in Beihang University. He has been teaching as the dean of studies at Beihang University since 2011. His current research interests include satellite navigation and satellite communication.

Wang Zulin received Ph.D. degree in communication and information system from Beihang University, Beijing, China. He is a professor and dean of School of Electronic and Information Engineering, Beihang University. His current research interests include signal processing and avionics electronic system.